# Laser-Based Cell Printing

Lothar Koch, Andrea Deiwick, and Boris Chichkov

## Contents

### Abstract

The development of reproducible well-defined 3D cell models is a key challenge for the future progress in tissue engineering. The structural dimensions in natural tissue are significantly lower than 100 μm. Thus, the ability to precisely position different cells in complex 3D patterns is of essential importance, even if it is not fully determined which precision or resolution is really required.

L. Koch (✉) · A. Deiwick · B. Chichkov
Laser Zentrum Hannover e.V., Hannover, Germany
e-mail: l.koch@lzh.de; a.deiwick@lzh.de; b.chichkov@lzh.de

This chapter discusses laser-based techniques for printing living cells in two- or three-dimensional patterns. One method known as laser-guided direct writing has been used to position individual cells in a cell medium bath by applying the laser optical tweezer technique.

A more common method applies the laser-induced forward transfer (LIFT) for cell printing. For this method, many different designations are used like biological laser printing (BioLP), laser-assisted bioprinting (LAB, LaBP), or matrix-assisted pulsed laser evaporation - direct write (MAPLE-DW). There are also some technical differences in the realization of cell printing with this method that are discussed in this chapter. Applications like printing of multicellular arrays, stem cell grafts, and tissue as well as in situ printing will be presented.

# 1    Introduction

In principle, the field of bioprinting can be separated in printing of scaffolds and patterns of molecules and biomaterials, randomly seeded with cells after printing if applicable, and printing of cells and microorganisms. Laser-based techniques have been developed for both applications. While laser-based scaffold generation is described in chapter ▶ "Additive Manufacturing for Tissue Engineering" this chapter describes laser-based printing of vital cells.

The ultimate goal of bioprinting certainly is the ex vivo generation of fully functional organs from cultivated cells and biomaterials. Therefore, complex three-dimensional (3D) patterns of different cell types have to be printed, mimicking tissue structure, often including a perfusable vascular network. The distance between adjacent vessels in some tissue well supplied with blood like liver is partly below 200 μm with the size of microvessels down to 10 μm. Since the size of most human cells is about 10 μm, the printing resolution for tissue printing should be in the lower double-digit micron range.

For printing, cells are mostly embedded in a sol, the non-gelled precursor of a hydrogel, often referred to as bio-ink, and deposited at their designated position in a droplet or strand. For 3D printing, the sol is gelled after printing to achieve an adequate stiffness.

Mainly three different techniques are applied to bioprinting (Ringeisen et al. 2006; Hon et al. 2008): ink-jet printing, extrusion printing (also referred to as robotic dispensing, bioplotting, syringe-based printing), and laser-assisted bioprinting (LaBP, also referred to as laser-induced forward transfer, biological laser printing, laser bioprinting, matrix-assisted pulsed laser evaporation - direct write (MAPLE-DW)). Ink-jet and extrusion printing are nozzle-based techniques, while LaBP is nozzle-free. Inside nozzles, cells undergo mechanical stress due to shear forces which are dependent on velocity and viscosity of the sol as well as nozzle diameter and cell density. To achieve a high resolution, a small nozzle diameter is required. However, if the nozzle diameter is not much bigger than the cell size, viscosity and cell density or velocity needs to be low.

Ink-jet printing requires certain velocity and applies typically nozzle diameters below 100 μm. This allows printing of droplets with very small volumes at high repetition rates

(chapter ▶ "Inkjet Printing for Biofabrication"). However, only low cell densities (typically $10^6$/ml, compared to $10^8$/ml for LaBP) and low-viscosity materials (typically lower than 10 mPa · s, compared to 1 Pa · s for LaBP (Lin et al. 2009)) are printable.

With extrusion printing (chapter ▶ "Extrusion-Based Biofabrication in Tissue Engineering and Regenerative Medicine"), the biomaterial is pressed (extruded) through a nozzle as a strand. Therefore, nozzles with inner diameters between 50 and 1000 μm are used. To achieve sufficient printing velocity with small nozzles, only low-viscosity materials and low cell densities might be printed, comparable to ink-jet printing. Therefore, usually nozzles with diameters between 500 and 1000 μm are applied, resulting in relatively low printing resolution not sufficient to print complex microvascular networks. With bigger nozzle diameters, sols with high viscosity and embedded high cell density can be printed.

LaBP as a nozzle-free technique is capable of printing small droplets comparable to ink-jet printing and printing highly viscous sols and high cell densities comparable to extrusion technique. The advantage of LaBP is that printing of high cell densities and highly viscous materials can be combined with high resolution. With LaBP, more than 100,000 cells per second can be printed with high cell survival rate. Printed tissue with tens of millions of cells already has been demonstrated. However, each of the aforementioned printing techniques has its individual advantages and drawbacks and may be preferred for specific applications.

## 2 Laser-Based Cell Printing Techniques

### 2.1 Laser-Guided Direct Writing

While LaBP is the laser-based technique most commonly applied for cell printing, it is not the only one. A method based on the optical tweezer effect, usually referred to as laser-guided direct writing (LGDW), was used by Odde and Renn (1999), to arrange cells in two- and three-dimensional patterns without a sol or hydrogel.

The peculiarity of LGDW compared to most other cell printing techniques is the absence of a sol as bio-ink and droplet or strand formation. Cells swimming in cell culture media are trapped by a laser beam and moved slowly to their designated position on a surface. Therefore usually coherent wave lasers are applied. Cells get into the laser beam more or less randomly and act like a convex lens due to their spherical shape, translucence for the laser wavelength, and an index of refraction different from water. The laser photons are deflected by this lens, changing their momentum, which implies an opposite change in the momentum of the cell (conservation of momentum). This results in photon-induced movement of the cell (Fig. 1). While the photon is deflected toward the cell's center, the cell is accelerated in the opposite direction. Since many photons interact with the cell at the same time, the cell moves toward the area with the highest cell density; typically this is the center of the laser beam. Additionally, photons reflected or absorbed by the cell transfer a momentum in the direction of the laser beam onto the cell. Therefore, the cell moves along the optical axis of the laser beam. With LGDW, the laser beam is directed onto a surface in the cell medium, and a cell is
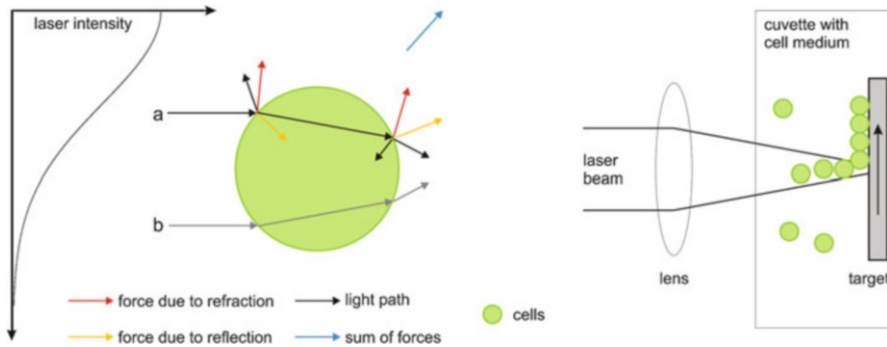
**Fig. 1** Schematic of the laser-guided direct writing technique similar to Odde and Renn (1999) (Copyright © 1999 Elsevier Science Ltd. All rights reserved). *Left*: Optical forces of the laser tweezer effect. Laser photons are reflected and refracted at each interface between cells and cell media, resulting in a redirection of the photons. Since photons have momentum, their redirection by interacting with the cell results in a corresponding momentum transfer to the cell. The sum of forces from interactions with a ray pushes the cell toward the (original) optical axis of the ray and along the beam axis. If the laser intensity varies over the cell–beam cross-section, the cell is pushed toward the region with the highest intensity (forces from stronger ray a overcome forces from ray b), which is in the beam's center in case of a Gaussian beam. Thus, the cell is pulled radially inward and pushed axially forward in the direction of the laser beam. *Right*: If the laser beam is weakly focused onto a target that is positioned in cell suspension, the cells are propelled to the focal spot and attach to the target's surface. By moving the target relatively to the laser beam, a line of cells can be written

propelled by the photons to this laser spot where it adheres. Now the laser is moved to another position to deposit the next cell on the surface or to cells already present at this position (analog to 3D printing).

LGDW offers an unbeatable resolution since it is a pure single cell printing technique without any surrounding bio-ink, enabling printing of 3D structures consisting of cells only.

However, this technique is extremely slow, since the photons need to push the cell against the fluid resistance of the cell media; Odde and Renn (1999) achieved a cell velocity of 10 μm (a typical cell diameter) per second which implies printing of fewer than one cell per second. Therefore, this technique is suitable for positioning of a few cells in well-defined patterns with precise distances, also in 3D, but not for printing tissue with millions of cells. LGDW is therefore rarely used nowadays and will not be considered in the following.

## 2.2 Laser-Induced Forward Transfer

More common is LaBP, adapting for cell printing a technique called laser-induced forward transfer that is used for electronic circuits, for example, electrodes on solar panels. The principal setup for LaBP applies a pulsed laser and a substrate transparent for the laser wavelength. Usually, the substrate is a glass slide (e.g., 1 mm thick) or fused silica for UV lasers. Most often, it is coated with a thin layer of material that
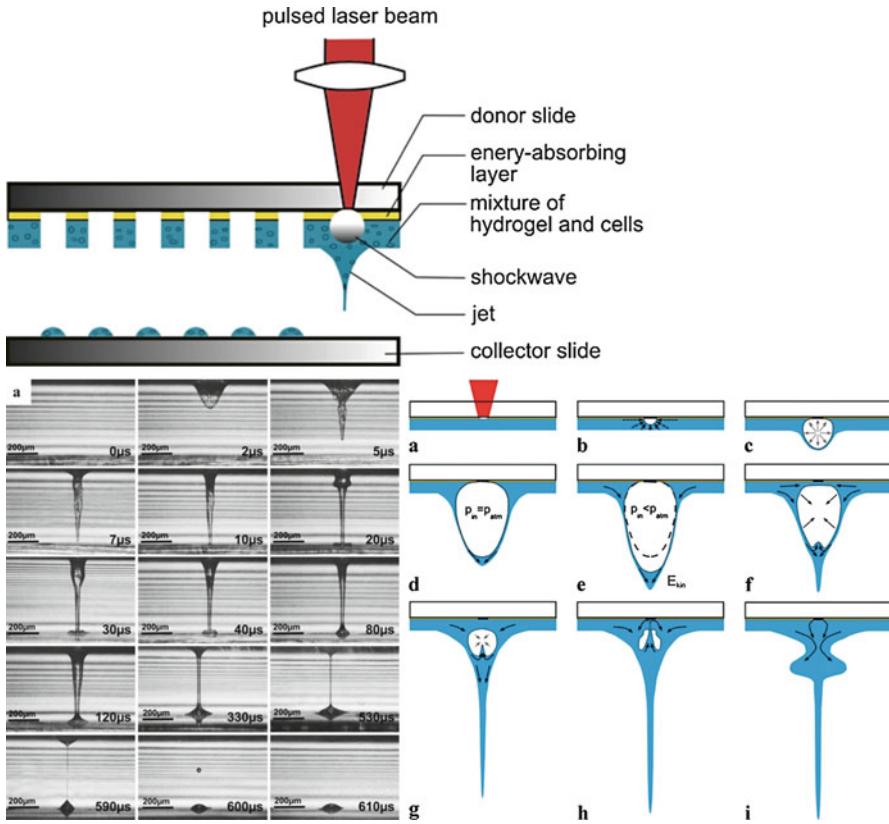
**Fig. 2** Schematic LIFT setup for hydrogel printing; time-resolved images of the hydrogel jet formation during LIFT; scheme of the bubble dynamics and jet formation during LIFT. *Gray arrows* indicate expansion or contraction of the vapor, *black arrows* mark flows, and *dashed arrows* resistance of the hydrogel against vapor bubble expansion (Reprinted from Unger et al. (2011) Copyright © 2011 Springer-Verlag)

absorbs the laser radiation. Onto this layer, the bio-ink to be printed is spread, usually a sol with embedded cells.

The substrate is mounted upside down into the printing setup (Fig. 2), and the laser pulses are focused through the transparent substrate into the absorption layer (also referred to as dynamic release layer).

The electrons in this layer absorb the laser photons. Thereby, plasma is generated within tens of picoseconds. This plasma is further heated by laser irradiation. Thereby, the absorption layer is evaporated in the focal spot, and a vapor bubble is generated. Since this bubble was generated at the glass slide surface (Fig. 2), it expands into a half-space. The resistance against bubble expansion is lowest perpendicular to the surface, because in this direction the amount of sol to be pushed aside is small compared to the lateral one. Therefore, the vapor bubble expands in an elongated shape. The stretching of the sol layer initiates a flow inside this layer.

While the vapor bubble expands, the inner pressure decreases below the atmospheric pressure, resulting in a re-collapsing of the bubble within a few microseconds after the laser pulse impact. However, the sol at the forefront of the bubble moves on due to inertia, surface tension, and the bubble collapsing from the sides and forms a sol jet that is fed further by the sol flow lasting for some hundred microseconds (Unger et al. 2011). For printing, the glass slide is positioned in a short distance above an object to print onto. The sol flows via this jet to a spot on the surface of this object. The sol jet disrupts after a few hundred microseconds due to a limitation of the sol "reservoir," springing from an area on the glass slide with about 200 μm in diameter. The sol remains as a droplet on the object. Each laser pulse is focused on a new spot on the absorption layer. By moving the substrate and repositioning the laser focus, every desired two-dimensional pattern can be printed, and layer by layer also 3D patterns can be generated. Cells have been printed onto different objects like glass slides, sheets of different materials (see below), and heart valve leaflets (Klopsch et al. 2012) and into scaffolds (Ovsianikov et al. 2010).

## 3    Applied Materials and Lasers

For cell printing, a wide range of absorption materials, bio-inks, and laser parameters are applied. For some absorption materials, certain wavelength ranges are required; polymers, for example, often require applying ultraviolet lasers. Here, an overview of the laser wavelengths and pulse durations, the absorption materials, and bio-inks that have been used by different groups will be given, which, however, does not claim to be exhaustive.

### 3.1    Dynamic Release Layer

The most widely used group of absorption materials are thin layers (about 10–100 nm thick) of metals like gold (Dinca et al. 2007), silver (Hopp et al. 2005), and titanium (Duocastella et al. 2010a), usually applied by sputter coating. They are combined with a wide range of laser wavelengths. Sputter coating of these metals is well established with high reproducibility and relatively cost efficient. Due to the surface properties of metal absorption layers, sol layers can be applied quite homogeneous and reproducible on them. The disadvantage of metal layers is the generation of debris. Ions, clusters, and micro- and macroscopic particles will be printed together with the bio-ink. This is not necessarily problematic with gold and titanium (oxide) as inert biocompatible materials; the debris is not toxic for the cells (see paragraph on process impact on cells below). Nevertheless, if thicker 3D structures are printed, the debris is clearly visible. If one day complete organs will be printed for implantation, this debris presumably cannot be tolerated.

Alternatively, polymer layers like 90–150 nm triazene (Palla-Papavlu et al. 2011), 7 μm polyimide (Brown et al. 2012), 1.35 μm polyethylene naphthalate foil (Vogel et al.

2007), gelatin layers (Schiele et al. 2011), or a two-layer system (10 μm cyanoacrylate + 25 μm brass foil (Lin et al. 2011)) have been used for different purposes.

Triazene is expected to be transferred completely into gaseous reaction products by ultraviolet laser irradiation. Thus, the debris problem would be avoided. However, there still might be a small amount of debris and maybe some altered chemical substances are generated that are embedded in the printed structure.

To completely eliminate the debris problem, Lin et al. (2011) investigated a two-layer absorption system with an adhesive cyanoacrylate layer on the glass slide and a brass foil on top. The laser pulse evaporates the cyanoacrylate only, and the vapor bubble bulges the brass foil without disrupting it. By using a relatively thick 7 μm layer of polyimide and an ultraviolet laser with 355 nm wavelength, Brown et al. (2012) realized this so-called blister effect with a single layer. The laser pulse vaporized the polyimide layer only partially near the substrate, while the absorption layer surface opposite to the substrate remains intact. The vapor bubble at the substrate polyimide interface only bulges the non-vaporized part of the absorption layer. This bulging or blister effect transferred enough momentum into the bio-ink to induce jet generation and the printing of the bio-ink.

Sometimes, systems without an absorption layer (e.g., Barron et al. 2004) are used. Thereby, the biomaterial to be printed also serves as laser-absorbing material; a small part of it is vaporized thereby. However, the biomaterial not necessarily has good optical properties for absorbing laser radiation. Furthermore, focused laser radiation, especially in the ultraviolet range, potentially harms cells.

## 3.2    Bio-ink

For printing 3D cell patterns or tissue, mostly the cells are suspended in a bio-ink, which is usually a sol or a mixture with a sol component. To achieve three-dimensionality, a certain stiffness of the bio-ink after printing is required. For the printing process itself, a viscous sol but not a stiff gel has to be used; therefore, the gelling should occur after printing. For printing of 2D cell patterns, stiffness is not required, and even printing of cells suspended in pure culture media is possible. Furthermore, the bio-ink needs to support cell survival. Therefore, nontoxicity, a neutral pH value near 7.4, a suitable temperature, and permeability for oxygen and nutrients are prerequisites, but some cell types have further demands like peptides to adhere to. Furthermore, bio-inks might induce stimuli to the cells, which are not always desirable. Typically, these different aspects are addressed by different components of a sol mixture.

In general, the mixture consists of four components. One component offers a suitable environment with nutrients for the cells; a second component is added for optimized viscosity. Depending on the application, stimuli like growth factors or agents are added. This sol mixture is printed with embedded cells and gelled with a cross-linker. The cross-linker may be printed in a second step or can be sprayed onto the printed sol. Alternatively, the sol can be printed directly into a cross-linker reservoir (Yan et al. 2013).

For LaBP, sols and hydrogels with a wide range of rheological properties (Lin et al. 2009; Gruene et al. 2011a) have been applied. As one example, alginate (1–6% w/v) provides a suitable viscosity for printing and gels by adding calcium ions. For cell-friendly environment, blood plasma might be added. After printing alginate mixed with plasma and cells, calcium chloride solution is sprayed on the printed pattern for gelation.

A second example is fibrin gel, which is generated by the human body to close wounds. The gelation is started by mixing fibrinogen with thrombin. Both provide a cell-friendly environment, but their viscosity is below the optimum for printing. Therefore, fibrinogen is printed mixed with cells and hyaluronic acid, which has a higher viscosity and can also be found in the human body. As the next layer, thrombin is also printed mixed with hyaluronic acid and cells. Thereby, fibrinogen and thrombin from succeeding layers gel and stiffen the printed structure. By the way, fibrin is also an example of undesired stimuli. It stimulates keratinocyte cells to migrate. If printed within fibrin, keratinocytes reorganize in the printed structure and can be found later in completely different formations than the printed one.

Collagen is a further gel of interest, since it is the most abundant protein in the human body. However, the collagen sol is acidic, and therefore, cells inside would die quickly. Thus, it does not allow a post-print gelling. For neutralization, collagen needs to be mixed with a base to yield a physiological pH value of 7.4 and a buffer, before adding cells. Thereby, collagen starts to gel. Depending on temperature and concentration, the gelling process takes some minutes. The gelling process is typically inhomogeneous, with a viscosity changing over time and varying locally by differently advanced gelling. Thus, printing is possible with reduced resolution only, if the neutralized collagen is printed during the gelling process. For printing 3D constructs mainly from gels like collagen, where the gelling occurs by a change of the pH value, the ability of printing high viscosity gels is required.

It is the dynamic viscosity that is important and which may differ significantly from the static viscosity. The viscosity dependence on the shear velocity is material specific. Since shear forces can destroy cells, shear-thinning sols are advantageous. Their viscosity decreases when propelled forward by the vapor bubble and in the sol jet, inducing lower shear forces to the cells. Shear-thickening sols would be problematic. Alginate and hyaluronic acid are shear thinning.

## 3.3    Laser Parameters

In addition to diverse laser absorption materials, also lasers with different parameters have been applied for LaBP. The wavelengths range from 193 to 1064 nm, and the pulse durations are mostly in the nanosecond domain (see Fig. 3). Furthermore, focusing optics with different focal length and spot sizes and different laser pulse energies are applied.

Most groups printing cells by LaBP use ultraviolet lasers with pulse durations from 3 to 30 ns and 193 nm (Palla-Papavlu et al. 2011; Lin et al. 2011), 248 nm (Pirlo et al. 2011; Dinca et al. 2008), 266 nm (Othon et al. 2008), 337 nm (Vogel et al. 2007), or

**Fig. 3** Pulsed lasers with a wide range of parameters are used for laser-assisted bioprinting. Typically, the pulse duration is in the range from 1 to 30 ns, while the wavelength is in the ultraviolet (from 193 to 355 nm) or in the infrared (1027 or 1064 nm) range
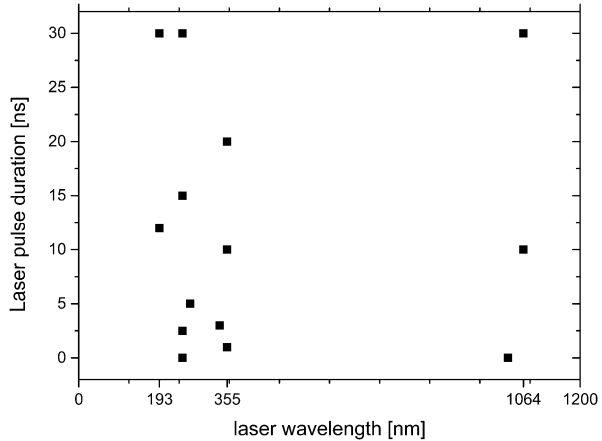
355 nm (Duocastella et al. 2010a; Brown et al. 2010) wavelength. UV lasers are used in combination with all mentioned laser-absorbing materials. They are advantageous for polymeric absorption materials, since single UV photons have enough energy to induce chemical reactions. Thus, they break up solid polymers and convert them into gaseous substances – ideally completely. On the other hand, UV radiation with wavelengths below 300 nm is also used for sterilization and may be harmful to cells.

As an alternative, near-infrared (NIR) lasers with 10 or 30 ns pulse duration and 1064 nm (Catros et al. 2012; Koch et al. 2010) wavelength have been used in combination with metallic absorption layers (gold, titanium). Duocastella et al. (2010b) printed a glycerol-water blend with 1027 nm wavelength and 450 femtosecond pulse duration.

Mostly, near-infrared lasers are combined with metal (gold, titanium) absorption layers, causing debris deposition in the printed structure. However, metal absorption layers are advantageous for most evenly spreading biomaterials on the absorption layer surface.

In spite of these wide ranges of applied laser parameters, so far their impact on the transfer process has hardly been analyzed in direct comparison with the exception of laser pulse energy. There is one publication, in which Dinca et al. (2008) laser-printed proteins and DNA but not cells with 500 fs pulse duration at 248 nm wavelength and compared the results with those achieved with 15 ns pulse duration. As a result, applying ultrashort laser pulses with 500 fs pulse duration allowed printing of significantly smaller droplets.

## 3.4    Controlling the Droplet Volume

Several parameters determine the volume of droplets printed by LaBP. Obviously, the achievable droplet volume depends on laser pulse energy and focal spot size, but it also depends on the bio-ink's viscosity and surface tension and on the thickness of the laser absorption layer and the bio-ink layer.

Sometimes it is aspired to print droplets as small as possible to achieve high resolution. However, going to the limit increases the risk that inhomogeneity of the bio-ink layer on the donor may lead to missing droplets, which are not printed from positions where the bio-ink layer is a bit thicker. Therefore, the intended droplet size needs to be a bit above the limit, and the homogeneity of the bio-ink layer is very important for a good printing result. Besides layer thickness homogeneity, also homogeneity of the bio-ink composition and viscosity is important.

In general, there are three laser pulse energy domains. Below a certain threshold (lower limit), there is no material transfer; though a vapor bubble is generated and there might be a jet formation as well, the bio-ink will remain at or return to (if a sol jet is formed) the donor slide due to the surface tension. Above an upper limit, the vapor bubble will not re-collapse but burst, causing strong splashing with the deposition of several droplets in an irregular pattern on the acceptor.

In the energy domain of interest between these limits, a jet dynamic occurs leading to the deposition of a single droplet at a predefined position. In this energy domain, the droplet volume increases with the laser pulse energy in a nearly linear correlation. Of course, besides the laser pulse energy, also the laser focus area is of importance for the printed droplet volume.

The dependence of the printed droplet volume on viscosity and thickness of the bio-ink layer is more complex. A thicker layer usually results in bigger droplet volume at the same laser pulse energy, if there are printed droplets at all. In contrast, there is no systematic dependence of droplet volume on the viscosity at different laser pulse energies. The droplet volume increases with rising viscosity until a maximum value is reached and decreases with further rising of the sol's viscosity (Gruene et al. 2011a). With an increased sol layer thickness, this effect is even more pronounced. The specific viscosity, at which the printed droplet volume reaches its maximum, reduces with a lower thickness of the sol layer. Depending on the printed material, the volume of a printed droplet can be in the range of sub-picoliter (Baum et al. 2013) to several nanoliters and more.

Examples of laser-printed cell patterns with different droplet volumes are shown in Fig. 4. The quantity of cells per droplet is usually dependent on the cell density in the sol layer and the droplet volume and is subject to statistical variations.
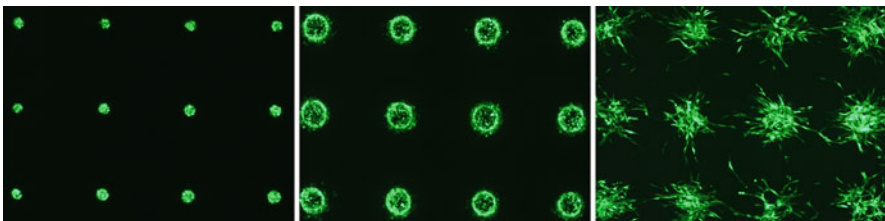


**Fig. 4** Dependence of the droplet volume on laser pulse energy (*left*, 20 μJ; *middle*, *right*, 30 μJ): Printed droplets with transduced fibroblasts (GFP labeled NIH3T3) embedded in a 3:2 mixture of fibrinogen and hyaluronic acid and printed onto a layer of fibrin, imaged directly after printing (*left*, *middle*) and after 2 days (*right*). Distance between adjacent droplets is 500 μm

Alternatively, droplets containing single cells might be printed, but this requires a low cell density and is time consuming, since each cell needs to be targeted separately.

## 4       Process Impact on Cells

Successful cell printing was reported by several groups with various kinds of cell types and different laser printing setups. For applying bioprinting techniques, it is crucial that cells are not affected by the printing process. This implies that the printed cells maintain their vitality and behavior and their phenotype and genotype and that stem cells retain their differentiation potential. Therefore, the impact of the printing process on cells and especially stem cells was extensively investigated.

Directly after printing the cell vitality was determined. Several groups (Barron et al. 2005b; Hopp et al. 2005; Koch et al. 2010) reported near 100% post-printing cell viability with different lasers, absorption layers, and cell types.

It was further investigated if the mechanical forces during printing might induce DNA strand breaks, which potentially could induce a medium-term degradation of the cell not directly visible after printing. This genotoxicity was investigated via a single cell gel electrophoresis (comet assay), and it was demonstrated that the printing process does not induce DNA strand breaks (Ringeisen et al. 2004; Koch et al. 2010). Thus, the genotype of printed cells is not affected.

Since high temperatures are generated locally in the plasma and the vapor bubble, cells potentially may be damaged by heat. Theoretically, the laser pulse's energy of a few ten micro-joules is sufficient to heat up a hundred picoliter (a typical droplet volume) from room temperature to a temperature above 42 $^{\circ}$C in which cells may be harmed. Therefore, it was analyzed via immunocytochemical studies (Barron et al. 2005a, b; Gruene et al. 2011b), if the printed cells express a so-called heat shock protein; no increased expression was observed.

As a further parameter of possible cell death in the aftermath of LaBP, Koch et al. (2010) assessed apoptosis by measuring the activity of caspases 3/7 up to 48 h after printing of cell lines and human mesenchymal stem cells (hMSC). No increase in apoptosis was detected, neither compared to nonprinted control cells nor compared at different test intervals.

Additionally, the effect of the printing process on cell proliferation was studied by cell counting up to 6 days after printing. In accordance with experiments of other groups on other cell types (Barron et al. 2005b; Hopp et al. 2005), no difference in the proliferation behavior of cell lines and stem cells compared to nonprinted control cells was observed (Koch et al. 2010).

Since stem cell differentiation can be induced by mechanical forces, it is important for the printing of stem cells that the printing does not affect their differentiation potential and behavior. In a flow cytometric analysis of the immunophenotype of human mesenchymal stem cells (hMSC) 4 days after printing, Koch et al. (2010) observed no significant difference in the ratio of expression of typical MSC-marker

proteins on the printed cells versus control cells; the immunophenotype was not influenced. The influence of laser printing on the differentiation behavior of MSCs was studied by Gruene et al. (2011b, c). No difference was observed between the printed and nonprinted stem cells in their differentiation behavior toward different lineages.

Summing up, so far all studies consistently stated that the laser printing procedure with suitable parameters does not affect the cells; they are vital and fully functional.

## 5    Applications

Besides studying fundamental aspects of LaBP, like the effect of laser parameters, absorption layer material and thickness, or bio-ink material mixtures, viscosity, layer thickness, and cell density, also different applications were tested. Such application studies have two aims. Of course, the printing technique itself needs to be tested, but it is also necessary to investigate the principal requirements for printing biological systems like tissue.

So far, it can only roughly be estimated, which printing resolution is actually needed for generation of complex tissue, since it is not well known, how to make the cells establish the desired structures like vascular networks or nerves, for example. Since the cells are spherically shaped when printed with the bio-ink between them, there is always some self-organization of the cells required for tissue generation. During some time after printing, there is a cellular migration and arrangement due to stimuli from surrounding cells and the chemical and mechanical cues from the bio-ink, maybe as a cross-linked hydrogel. These stimuli and cues need to be considered or – better – harnessed for generating a specific cell construct or tissue. Thus, the printing pattern does not necessarily need to be (or even should not be) exactly like the tissue to be generated. This is sometimes referred to as "4D printing" with time and cell organization as the fourth dimension. To understand how exact cells need to be printed in a specific position, to make them fulfill the intended function, requires further extensive studies. This is true not only for LaBP but for all cell printing techniques. However, LaBP is particularly suitable for such studies due to its versatility.

Many different studies on applications of LaBP have been published so far, of which an overview will be given in the following. Really complex tissue, especially with an integrated perfusable vascular network, has not been printed so far. Nevertheless, first steps in this direction have already been taken. Different laser-printed 3D cell constructs are presented below, defined 3D spot arrays for microscopically observation of cell–cell interactions, a monocellular 3D stem cell graft, a multicellular 3D skin equivalent, stackable biopapers with printed cells, and in situ printing of cells into mice.

## 5.1    Printed Stem Cell Grafts

Stem cells are very interesting for regenerative medicine due to their self-renewal and differentiation ability. These abilities are regulated by cell density, cell–cell contacts, cell–matrix adhesion, and the exchange of growth factors and oxygen in the cell's 3D microenvironment (Discher et al. 2009), also referred to as stem cell niche. Therefore, one important application for cell printing technologies would be fabricating 3D in vitro models mimicking such cell niches for studying cell behavior under predefined conditions more complex than conventional 2D cell cultures but more controllable than in vivo models.

The ability of LaBP for generating such 3D environments was demonstrated by Gruene et al. (2011b, c). They printed 3D patterns of mesenchymal stem cells (MSCs), approximately 300 μm high, for studying, if the differentiation potential toward different lineages of these stem cells (porcine bone marrow-derived (pMSCs) and human adipose-derived MSCs (ASCs)) was affected by the printing process and if these stem cell grafts can be differentiated within the printed pattern.

MSCs can be found in many adult tissues and represent an attractive cell source due to their high proliferation capacity, self-renewing ability, and their mesodermal differentiation potential. MSCs are expected to regenerate many tissues, like bone and cartilage. Therefore, these cells are very attractive for tissue engineering applications.

For printing, the MSCs are embedded in a natural sol of autologous origin consisting of alginate and ethylenediaminetetraacetic (EDTA) blood plasma. Each printed layer was cross-linked with calcium chloride, to form a hydrogel as extracellular matrix for the grafts. This material is compatible with the cells and enables the exchange of nutrients and soluble factors. Thereby, material elasticity and forces have to be considered, since these parameters are known to influence stem cell differentiation (Hellström et al. 1999). Additionally, the differentiation of stem cells is dependent on cell density; in particular, chondrogenesis requires a high cell density. Therefore, for generating stem cell grafts, printing with defined, variable, and high cell density is required (Hui et al. 2008; Takagi et al. 2007).

Stem cells may undergo forces during the printing procedure that would not affect their proliferation ability but might induce uncontrolled differentiation (Clause et al. 2010). To screen out such negative effects of LaBP on stem cell behavior, several quantitative and qualitative investigations were carried out, showing that the differentiation potential of MSCs into osteogenic, adipogenic, and chondrogenic lineages is not affected by the printing procedure, and the printed MSC grafts can be differentiated toward bone, cartilage, and adipose tissue (Fig. 5). Accumulation of calcium phosphate shows osteogenic differentiation, lipid vacuoles indicate adipogenic differentiation, and collagen type II is specific to chondrogenesis.

Additionally, LaBP enables printing of cell densities high enough for the promotion of chondrogenesis. 3D scaffold-free autologous tissue grafts can be fabricated with LaBP, keeping their predefined shape even after several weeks in culture and also after removal of the alginate matrix material after 2 weeks in culture (Gruene et al. 2011b, c).
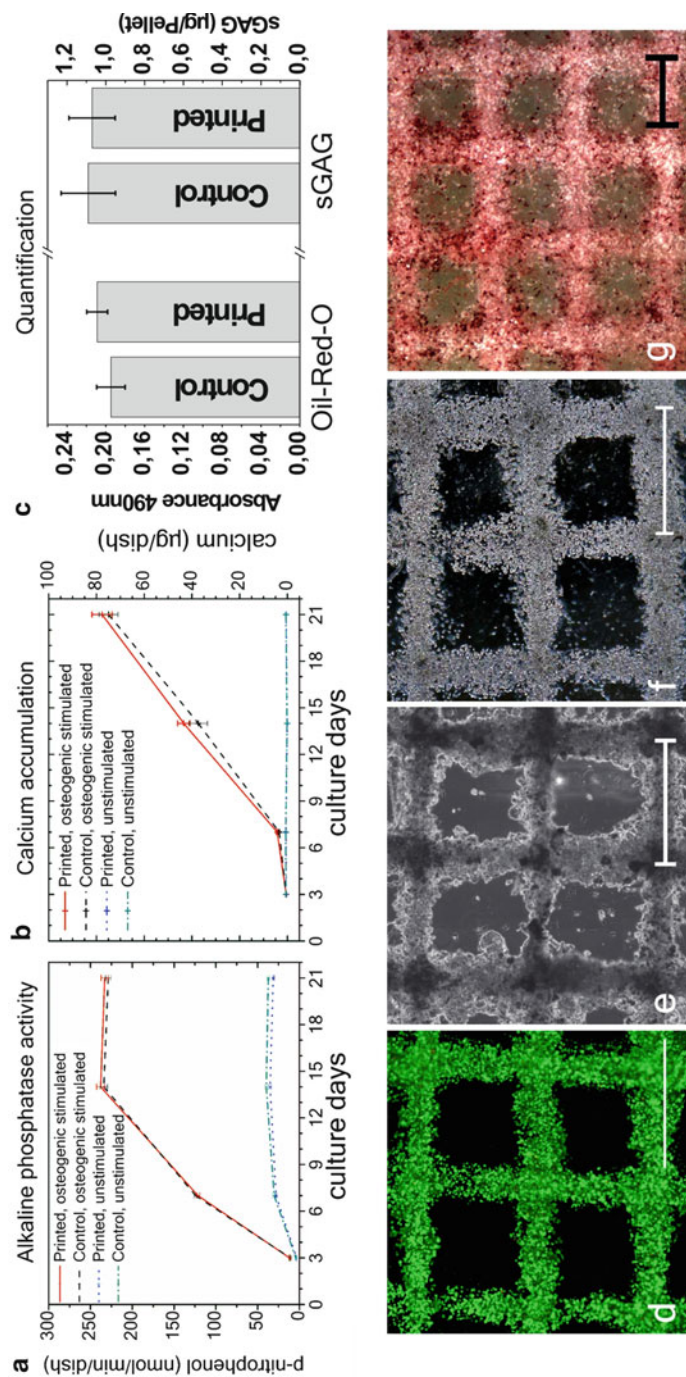
**Fig. 5** Osteogenic, adipogenic, and chondrogenic differentiation potential of printed and nonprinted (**control**) mesenchymal stem cells (MSCs): (**a**, **b**) Quantitative assessments of (**a**) alkaline phosphatase activity and (**b**) calcium accumulation over a period of 21 days from printed and nonprinted control MSCs under osteogenic differentiation conditions in contrast to unstimulated stem cells (MSCs). Values are given as mean ± SEM (n = 8). (**c**) *Left:* The quantity of the lipid accumulation from printed and nonprinted control cells after 21 days under adipogenic culture conditions was determined by Oil Red O staining and radiation absorbance at 490 nm wavelength. *Right:* Quantitative indication of sulfated glycosaminoglycans (sGAG) for chondrogenesis, by the 1.9-dimethyl-l-methylene dye-binding assay after 21 days under chondrogenic culture conditions. Values are given as mean ± SEM (n = 5). (**d–g**) Printed 3D grid

## 5.2    Printed Multicellular Arrays for Cell–Cell Interaction Studies

Cellular microarrays have been developed for investigating cell responses in multiple parallel experiments (Fernandes et al. 2009) and to enable reproducible studies of the effects of proteins, growth factors, biomaterials, and drugs as well as the presence of other cells. Several studies indicate that cell behavior and tissue functionality are influenced or even controlled by local cell density, cellular spacing, cell–cell communication, and binding of cells to their 3D environment (Discher et al. 2009). The effect of the 3D environment on cellular behavior could be studied in printed 3D multicellular arrays. To prove the suitability of LaBP for generation of such arrays, Gruene et al. (2011d) printed arrays of droplets containing either human adipose-derived stem cells (ASCs) or endothelial colony-forming cells (ECFCs). These cells were chosen for investigation of vascular network formation, since recent studies indicate that these cell types represent suitable cell sources for therapeutic revascularization of ischemic tissues and can support the new vessel formation in engineered tissue constructs (Merfeld-Clauss et al. 2010; Wu et al. 2007; Gaebel et al. 2011). It was expected that the secretion of VEGF by the ASCs, which is well known for the promotion of endothelial cell proliferation, would lead to the outgrowth of ECFCs toward the ASCs along the VEGF gradient, as it was reported by other groups (Mirsky and Cohen 1995; Akeson et al. 2010). The cells were printed in 2D patterns of printed droplets on layers of fibrin hydrogel, each droplet containing one of both cell types, fibrinogen, and hyaluronic acid. Cultivated after printing in vascular endothelial growth factor-free (VEGF-free) medium for 10 days, cell–cell interactions were observed in arrays of separate droplets with ASCs and ECFCs as well as monoculture cell arrays containing only ASCs or only ECFCs as control. In each case, four independent cell arrays were printed.

As depicted in Fig. 6, the ASCs showed strong migration activity after 72 h, while the activity of ECFCs was very low. In the co-culture, the ASCs migrated toward the ECFC droplets, whereas the ECFCs showed negligible activity. After the ASCs got in direct contact with the ECFCs between days 3 and 5 (Gruene et al. 2011d), the activity of ECFCs strongly increased, and both cell types together began to form vascular-like networks with big branches. These networks were not observable either in the ASC or the ECFC controls. In all four independent co-culture cell arrays, these networks were formed and remained stable for 2 weeks under culture conditions. However, their formation did not occur at the same time.

---

**Fig. 5** (continued) structure of MSCs: directly after printing (**d**), after 25 days under osteogenic (**e**), and after 21 days under chondrogenic (**f**), or adipogenic (**g**) culture conditions. Microscopic images with phase contrast (**e, f**), vitality staining (**d**, calcein AM), Oil Red O staining (**g**). Accumulation of calcium phosphate for osteogenic differentiation (**e**) and lipid vacuoles indicating adipogenic differentiation (**g**) can be seen (Reprinted from Gruene et al. (2011b) Copyright © 2011 Mary Ann Liebert, Inc. publishers and Gruene et al. (2011c) Copyright © 2010 IOP Publishing. Reproduced with permission. All rights reserved)
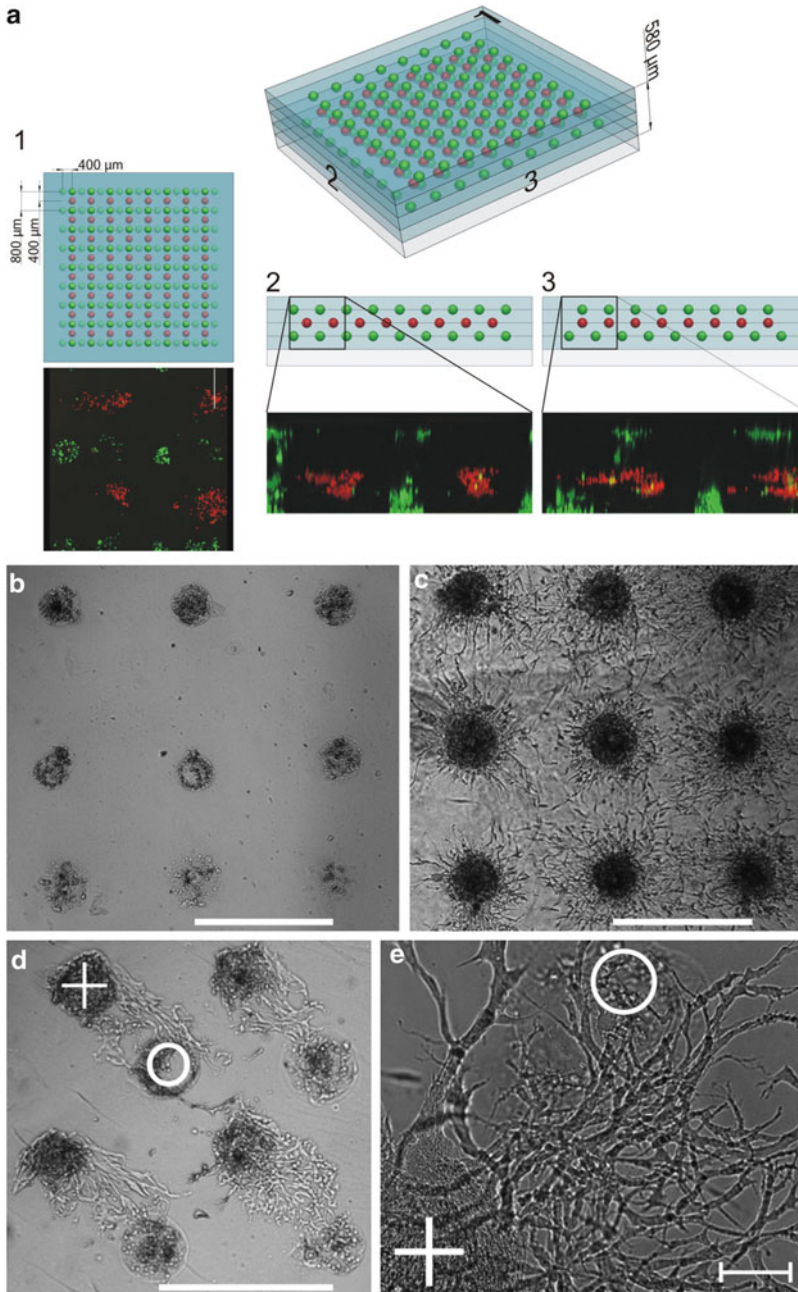
**Fig. 6** (**a**) Three-dimensional reconstruction of the 3D cell array by means of confocal laser scanning microscopy and the corresponding CAD model. ECFCs were stained with calcein (*green*), and ASCs were stained with TAMRA-5 (*red*). (**b–e**) Visualization of cell–cell interactions by 3D cell arrays in mono- and co-cultures, cultivated for 5 days under VEGF-free conditions.

The migration of ASCs toward ECFCs may be due to a gradient of platelet-derived growth factor (PDGF). The subtype PDGF-BB is expressed in large amounts by ECFCs and is well known for the stimulation of ASC proliferation and migration (Hellström et al. 1999).

Gruene et al. (2011d) also printed 3D cell arrays with the same cell types as a multilayer pattern. A hydrogel consisting of a fibrin precursor (fibrinogen) and hyaluronic acid served as the bio-ink and extracellular matrix material. First, a layer of fibrin is produced on a glass slide by blade-coating a fibrinogen layer and subsequent cross-linking with thrombin; second, different cell types are printed on top of these fibrin layers in droplets with a predefined spot spacing by LaBP; and third, a second fibrin layer is deposited on top using the same procedure. Then, the second and third steps have been repeated several times to produce true 3D cell arrays.

By printing spots of ASCs and ECFCs, they demonstrated that (i) cell spots can be arranged layer by layer in a 3D array; (ii) any cell–cell ratio, cell quantity, cell-type combination, and spot spacing can be realized within this array; and (iii) the height of the 3D array is freely scalable. The fibrin-based environment could be replaced by any other hydrogel. Printed cell arrays are a suitable tool for investigating such complex interactions between different cell types like vascular network formation in engineered tissue constructs. In another study (Taidi et al. 2016), droplets of alginate containing yeast (*Saccharomyces cerevisiae* var. *bayanus*) or algae (*Chlorella vulgaris*) have been printed and co-cultured to study the interactions between oxygen-consuming yeast and oxygen-generating algae colonies. Thereby, successful printing of microorganisms has been demonstrated.

## 5.3 Stackable Biopapers with Printed Cells

For the generation of 3D cell constructs thicker than the diffusion limit of a few 100 μm, the application of so-called biopapers was proposed as an alternative to directly print cell-containing gels layer by layer. Biopapers are flat substrates, sometimes spongy or scaffold-like, that are also referred to as sheets. Onto each biopaper, cells are printed in a two-dimensional pattern, and later the biopapers are stacked to generate a 3D structure and 3D assembly of the cells.

This concept has been combined with LaBP by Pirlo et al. (2011) and Catros et al. (2012). As spongy substrates, they used 300 μm thick poly(lactic-co-glycolic acid) (PLGA) scaffolds coated with Matrigel™ (now Corning Inc., NY, USA) and 100 μm thick electrospun polycaprolactone (PCL) scaffolds, respectively. As 2D patterns, they printed human umbilical vein endothelial cells (HUVEC) onto the

---

**Fig. 6** (continued) A *circle* indicates the printed ECFC spot and a cross the printed ASC spot. Interactions of ASCs and ECFCs (**d**, **e**) in comparison to separated arrays of ECFCs (**b**) and ASCs (**c**). A vascular-like network formation occurs after 5 days in the co-culture (**e**). Distance between spots with the same cell type is 800 μm. Scale bars are 250 μm (**e**) or 800 μm (**b**–**d**) (Reprinted from Gruene et al. (2011d), Copyright © 2011 Mary Ann Liebert, Inc. publishers)

Matrigel™-coated PLGA sheets and MG63 osteoblastic cells onto the PCL scaffolds, respectively. Later, they stacked these biopapers with printed cells to achieve 3D cell constructs. This technique enables cultivation of the 2D printed cells on the individual biopapers and cell formation with tissue-like intercellular junctions before stacking.

If generation of functional vascular networks on single biopapers is possible, this would be a very promising approach. The stacking of the biopapers could be carried out several days after printing, having enough time for vessel formation while the biopapers are in cell culture medium and the supply of cells with nutrients and oxygen is ensured. Stacking biopapers with functional vascular networks later would enable cell supply even in very thick 3D cell constructs. Additionally, requirements on the cell-embedding sol are reduced, since stiffness for three-dimensionality is not needed.

However, for generating predefined 3D patterns with high fidelity, precise stacking without any shift or rotation is essential. Furthermore, connections between cells and vascular networks of subsequent biopapers are required to achieve 3D tissue. Otherwise, cells would be involved in 2D cell patterns of single biopapers only, even if molecules like second messengers could diffuse through the biopapers. A further challenge would be to connect the vascular networks of several biopapers to some perfusion system. How far this method can be advanced remains to be seen.

## 5.4 Printed Skin Tissue

The major aim of cell printing is fabrication of functional tissues and organs with a wide area of application. Firstly, printed 3D patterns mimicking the placement of cells in specific tissues could improve our understanding of cell behavior, tissue functions, and regeneration. These complex interactions in 3D tissue and cell microenvironments in vivo cannot be simulated adequately with common ex vivo cell studies in two-dimensional cell cultures. Cell behavior differs radically in 3D.

Secondly, reproducibly printed 3D human tissue models can serve as test systems for studying effects and tolerability of chemical agents, cosmetics, or pharmaceuticals on tissues and organs. They could be integrated in so-called body-on-a-chip systems, more complex systems consisting of different tissue types combined in a micro-fluidic system. By using human cells, testing with such printed tissue models could even be more relevant than animal testing due to differences in the metabolism between animals and humans.

Of course, the ultimate goal of cell printing would be printing of complete human tissues and organs with full functionality as replacement organs for implantation to overcome the lack of donor organs. Organs, printed from autologous cells, someday may even outclass donor organs, since no rejection reaction is expected to occur and no livelong intake of immunosuppressant is needed.

Currently, research is far away from printing fully functional organs. For such organs an integrated perfusable vascular network would be necessary to supply the printed cells with oxygen and nutrients, if the tissue size is above a few hundred microns. The vascular networks of natural tissue consist of vessels with diameters

between 10 μm and a few millimeters. Such perfusable networks have not been printed so far.

However, basic tissue has already been printed. Koch et al. (2012) printed simple skin tissue consisting of two cell types, murine fibroblast (NIH3T3) and human keratinocyte (HaCaT from adult human skin) cell lines. This combination of well-established cell lines can be found in other studies (Bigelow et al. 2005), too. 3T3 fibroblast cells are widely used in the cultivation of keratinocytes, because they are secreting growth factors favorable for keratinocytes (Linge 2004).

Koch et al. (2012) printed these cells from 20 layers of fibroblasts and 20 layers of keratinocytes, both embedded in collagen type I, to mimic the layered structure of natural skin with dermis and epidermis (Fig. 7). Collagen was used as bio-ink in order to approximate native skin as good as possible, since it is the main component of the extracellular matrix in the skin. A collagen–elastin matrix (Matriderm, Dr. Suwelack Skin & Health Care, Billerbeck, Germany) was used as the basic substrate to print onto.

The main goal of this study was investigating tissue formation by cells after laser printing. Therefore, the existence of intercellular junctions, adherens junctions (Niessen 2007), and gap junctions (Mese et al. 2007) was observed. Such junctions can be found as cell–cell and cell–matrix connections in all kinds of tissue, abundantly in epithelium like the epidermis. Adherens junctions are fundamental for tissue morphogenesis and cohesion; they consist mainly of cadherins (calcium-dependent adherent proteins). Gap junctions are cell–cell channels that allow intercellular communication by passing chemical signals; they consist of connexins (Richard 2000) and are known to have a fundamental role in differentiation, cell cycle progression, and cell survival (Schlie et al. 2010).

In the printed skin tissue, the extensive formation of intercellular adherens junctions between printed keratinocytes and a minor formation between fibroblasts could be observed after 10 days. This is expected, since there is typically (Niessen 2007) a higher level of junctions in the dermal epithelium (epidermis), formed by keratinocytes.

The formation of gap junctions has also been observed in the cell membranes between all adjacent cells 10 days after printing. The functionality of cell–cell communication via gap junction coupling has been verified in vital 3D cell constructs with a dye-transfer method. Thereby, it has been demonstrated with respect to adherens and gap junctions that tissue-specific functions are developed by printed skin cells in collagen.

Furthermore, the formation of a basement membrane between keratinocytes and fibroblasts has been observed (Fig. 7), as it exists between epidermis and dermis in natural skin.

The same skin constructs have also been implanted into full-thickness skin wounds in nude mice, applying a dorsal skinfold chamber (Michael et al. 2013). They were fully connected to the surrounding tissue after 11 days. A multilayered epidermis has been formed by the printed keratinocytes with beginning differentiation and stratum corneum. Blood vessels have been detected to grow from the wound bed and the wound edges into the printed cells.
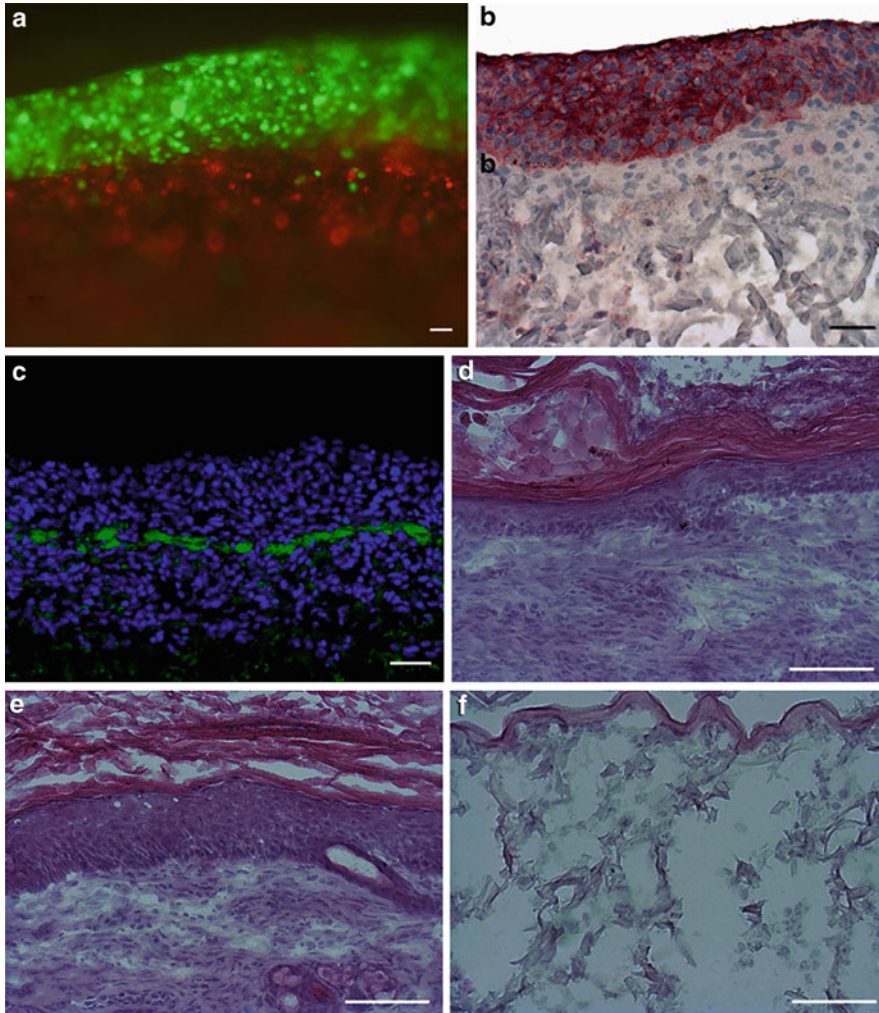
**Fig. 7** Laser-printed skin tissue mimicking its bilayered structure: Embedded in collagen type I, 20 layers of murine fibroblasts and 20 layers of human keratinocytes were printed subsequently on a collagen–elastin substrate. (**a**) Section through the laser-printed construct with transduced fibroblasts (*red*) and keratinocytes (*green*), prepared directly after printing. (**b**, **c**) Cryostat sections, prepared 10 days after printing. Immunoperoxidase staining of cytokeratin 14 (**b**) depicts keratinocytes in *reddish brown* in the bilayered structure while all cell nuclei (fibroblasts and keratinocytes) are stained with hematoxylin in *light blue*. Image (**c**) shows an anti-laminin staining in *green* and all cell nuclei in *blue* (Hoechst 33342). Laminin is a major constituent of the basement membrane in the skin. (**d**–**f**) Hematoxylin–eosin staining of paraffin sections, prepared after implantation for 10 days in dorsal skin of nude mice. Printed skin cells (**d**), on a collagen–elastin matrix; native dorsal mouse skin (**e**); the collagen–elastin matrix (**f**), implanted without cells, as a control. Scale bars are 50 μm (**a**–**c**) or 100 μm (**d**–**f**) (Partially reprinted from Koch et al. (2012), Copyright © 2012 Wiley Periodicals, Inc.)

However, natural mouse skin (Fig. 7e) is much more complex than the printed one (Fig. 7d). Figure 7f depicts Matriderm without printed cells after implantation for 11 days.

Actually no skin equivalent exists, which satisfactorily mimics native skins' functions (or appearance), like, e.g., the capability to control the body temperature with sweat glands, sensory skills, immunocompetence, or hair follicles. In future, LaBP might enable skin generation with all necessary cells in their specific microenvironment and the corresponding functions.

## 5.5    In Situ Printing

An alternative to implanting printed 3D cell constructs or tissue is printing cells directly into wounds or tissue defects. This has been demonstrated by Keriquel et al. (2010) by printing nano-hydroxyapatite (n-HA) slurry in mouse calvaria defect models in vivo. Hydroxyapatite is the major nonorganic component of bone and has been used in many studies on bone tissue engineering.

Two 4 mm diameter defects were generated with a trephine in the mouse skull. Into one defect the slurry has been printed, while the other one served as control. Thirty layers of the slurry containing n-HA and glycerol, with a thickness of about 20 μm each and 3 mm in diameter, have been printed layer by layer into one defect. Both defects were re-covered with soft tissue after printing.

After 3 months, in many defects with printed n-HA mature bone tissue has been observed, while bone repair has been incomplete in many mice's control defect (Fig. 8). However, from one mouse (sample) to another, bone regeneration was very inhomogeneous, and no statistical significance has been observed in bone repair enhancement by n-HA printing.

Besides the printing experiments, it has been investigated if tissue irradiated by infrared laser (1064 nm wavelength) during the printing might be harmed. Magnetic resonance imaging of directly irradiated dura mater, the outermost membrane enveloping the brain that is closest to the skull, displayed edema on the irradiated side after 1 week that has regressed after 2 weeks and has disappeared after 3 weeks. Therefore, it has been concluded that no deleterious effects are induced by the applied infrared laser on the brain tissue.

Although the experimental results have been heterogeneous and no cells have been printed, in vivo bioprinting has been successfully demonstrated. In vivo cell printing should be possible exactly the same way.

## 6    Discussion

Laser-assisted bioprinting (LaBP) has been applied for more than a decade for printing vital cells and different biomaterials in predefined two- and three-dimensional patterns.
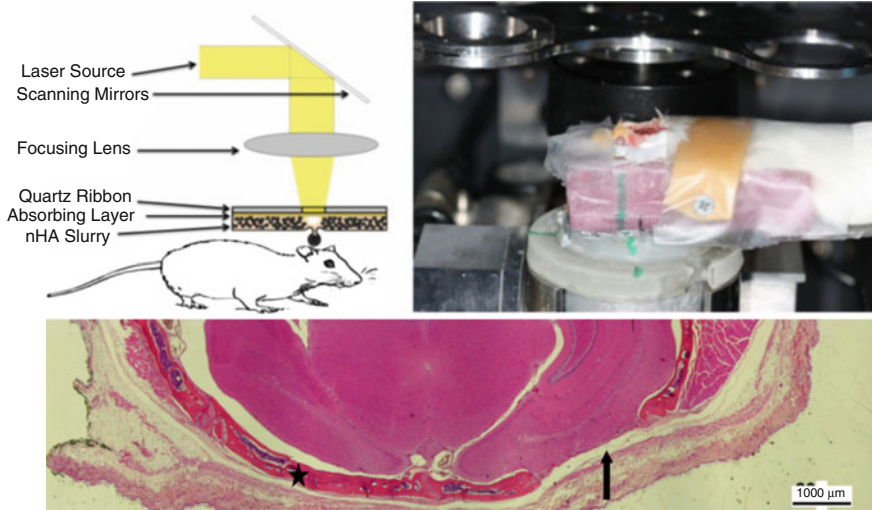
**Fig. 8** In situ bioprinting in mouse model: *Top*: (**a**) Schematic setup for in vivo laser printing; (**b**) specific holder for in vivo printing in mouse calvaria defects. *Bottom*: Complete bone repair on the test side was observed in one sample after 3 months (*star*). The bone defect control site is not reconstructed in this picture (*arrow*) (Reprint from Keriquel et al. (2010), Copyright © 2010 IOP Publishing. Reproduced with permission. All rights reserved)

Various cell types (cell lines, primary cells, stem cells) have been printed, and different studies have consistently demonstrated that this technique does not harm the printed cells or influence the differentiation potential of stem cells.

LaBP allows printing of (i) cell amounts ranging from single to hundreds of cells per droplet, (ii) sols (hydrogel precursors) with a wide range of rheological properties, and (iii) cells with micrometer resolution in a high-throughput manner. Besides cells, also microorganisms like yeast or algae, DNA, growth factors, or biological agents can be printed.

Different lasers with wavelength from ultraviolet 193 nm to infrared 1064 nm and pulse durations from 500 fs to 30 ns have been used, demonstrating that no specific laser parameters are generally preferable. There is also a broad range of materials that have been applied as laser absorption layers; however, some materials require a specific laser wavelength range, like ultraviolet radiation for some polymers.

The optimal absorption layer material has not been found so far. The requirements are (i) easy to be disposed on a laser transparent substrate, (ii) to offer surface characteristics that allow to blade-coat very homogeneous sol layers on it, (iii) no side effects on cells, and (iv) no debris generation by laser vaporization.

Additionally, many different bio-inks have been applied with a wide range of rheological parameters. Typically, this is a sol mixture that is cross-linked after printing, but also printing with cell media has been demonstrated. The bio-ink always needs to be chosen with respect to the cell type and desired tissue to be printed. Some cells are affected in their behavior by specific sols or hydrogels, and so

far there is not one bio-ink that fits for all applications. However, the choice of bio-ink has also an effect on achievable printing resolution.

Besides the development of the laser-assisted bioprinting technique itself and testing of materials for laser absorption and as bio-inks, a wide range of applications have been demonstrated.

Printing of stem cells for fabrication of 3D scaffold-free autologous grafts was shown. Mesenchymal stem cells have been printed in 3D patterns and differentiated toward different lineages (osteogenic, chondrogenic, and adipogenic) within their predefined structure. Especially, human adipose-derived stem cells offer large clinical potential for autologous tissue reconstruction therapies due to the ease of their withdrawal from adipose tissue and their ability to differentiate down the mesenchymal and non-mesenchymal pathway (Schaeffler and Buechler 2007).

For cell–cell and cell–environment interaction studies, LaBP was used to precisely arrange different cells in 3D spot arrays. As a proof of concept, interactions between endothelial cells and stem cells toward generating new blood vessels were investigated.

For proving the formation of tissue by printed cells, skin cells have been laser-printed in 3D multicellular constructs analogous to native skin archetype. The evolvement of intercellular adhesion and communication via adherens and gap junctions could be observed, which proves the tissue formation.

Reproducibly fabricated tissue equivalents could serve as 3D environments for studying cell behavior. By integrating further cell types, like endothelial cells for vascularization or dendritic cells in printed skin tissue for immune reactions, tissue equivalents may be developed further to their natural archetype. They could be used for testing cosmetics, pharmaceutical, or chemical agents reducing animal testing. Compared to animal testing, reproducibility of the printed skin tissue could become a significant advantage.

The tissue that has been printed with LaBP so far is relatively thin, which allows to supply cells with nutrients and oxygen by diffusion. For printing thicker tissue, a perfusable vascular network is required. This is the key challenge researchers are dealing with today in the tissue engineering field. Such a vascular network could be generated by printing blood vessel cells in a pattern integrated in the 3D printed structure. However, this network needs to be connected to an external pump and to be functional after a relatively short time period to supply the printed cells with nutrition.

For some tissue types, printing alone is not sufficient. If, for example, heart muscle tissue printing is intended, stimulation of the printed cell structure by mechanical forces is required, to induce a parallel orientation of the cells. A fabrication technique of very small cardiac tissue pieces already has been developed; for the fabrication of bigger tissue, it needs to be modified including the integration of a vascular network.

Additionally, for some organs even not all cell types are available, yet. Isolated from tissue and brought to conventional cell culture, cells may change their phenotype and lose their functionality. Some cell types still can't be cultivated outside their 3D microenvironment.

An alternative to scaffold-free printing of 3D cell constructs and tissue could be 3D stacking of biopapers, each with a printed 2D pattern on the biopaper surface. If a precise stacking is provided, this technique can enable the generation of well-defined 3D patterns within a 3D scaffold structure. Apart from some special scaffold geometries, this is not possible with conventional scaffolds, seeded with cells after fabrication. However, establishing vascular networks on 2D surfaces and integrating these 2D networks into a perfusable 3D vascular network will be very challenging.

Furthermore, direct printing into wounds of test animals was successfully tested. In the future, such an in situ printing might be applied in surgery for tissue repair, e. g., for cartilage or bone.

# 7 Conclusions

For generating replacement tissue and organs as well as cell-based therapies, an extensive understanding of interactions between different cells and their environment is essential. However, conventional cell studies ex vivo on two-dimensional cell culture plastic surfaces are limited significantly and are not appropriate to simulate complex interactions in cell microenvironments in vivo and in 3D tissue; cell behavior differs dramatically in 3D.

Thus, printed 3D cell models could enable better understanding of tissue-specific cell behavior and tissue regeneration. Really complex tissue, especially with an integrated vascular network, has not been printed so far. Nevertheless, first steps in this direction have already been taken. For future progress in tissue engineering, the development of reproducible well-defined 3D cell models is a key challenge. Since the structural dimensions in natural tissue are significantly lower than 100 μm, the ability to precisely position different cells in complex 3D patterns is essential.

There are other printing techniques under investigation, like techniques based on ink-jet printing, acoustic droplet ejection, or extrusion systems, which are described in other chapters of this book. Compared with them, laser-assisted bioprinting enables to print droplets of biomaterials (with or without cells) combining very low volumes with high viscosities (much higher than it can be done with the ink-jet printer or acoustic droplet ejection) and high cell densities. However, each technique has its advantages and disadvantages, and it is not clear yet if one technique will prevail in the future. Probably, there will be applications for all these techniques.

The ability of LaBP to precisely position various sols with a broad range of viscosities and high embedded cell densities in very small droplets is an important feature for future progress in printing complex tissue and organs.

# References

Akeson A, Herman A, Wiginton D, Greenberg J (2010) Endothelial cell activation in a VEGF-a gradient: relevance to cell fate decisions. Microvasc Res 80:65

Barron JA, Ringeisen BR, Kim H, Spargo BJ, Chrisey DB (2004) Application of laser printing to mammalian cells. Thin Solid Films 453–454:383–387

Barron JA, Young HD, Dlott DD, Darfler MM, Krizman DB, Ringeisen BR (2005a) Printing of protein microarrays via a capillary-free fluid jetting mechanism. Proteomics 5(16):4138–4144

Barron JA, Krizman DB, Ringeisen BR (2005b) Laser printing of single cells: statistical analysis, cell viability, and stress. Ann Biomed Eng 33(2):121–130

Baum M, Kim H, Alexeev I, Piqué A, Schmidt M (2013) Generation of transparent conductive electrodes by laser consolidation of LIFT printed ITO nanoparticle layers. Appl Phys A 111 (3):799–805. https://doi.org/10.1007/s00339-013-7646-y

Bigelow RLH, Jen EY, Delehedde M, Chari NS, McDonnell TJ (2005) Sonic hedgehog induces epidermal growth factor dependent matrix infiltration in HaCaT keratinocytes. J Invest Dermatol 124:457

Brown MS, Kattamis NT, Arnold CB (2010) Time-resolved study of polyimide absorption layers for blister-actuated laser-induced forward transfer. J Appl Phys 107:083103

Brown MS, Brasz CF, Ventikos Y, Arnold CB (2012) Impulsively actuated jets from thin liquid films for high resolution printing applications. J Fluid Mech 709:341–370. https://doi.org/10.1017/jfm.2012.337

Catros S, Guillemot F, Nandakumar A, Ziane S, Moroni L, Habibovic P, van Blitterswijk C, Rousseau B, Chassande O, Amédée J, Fricain J-C (2012) Layer-by-layer tissue microfabrication supports cell proliferation in vitro and in vivo. Tissue Eng Part C Methods 18(1):62–70

Clause KC, Liu LJ, Tobita K (2010) Directed stem cell differentiation: the role of physical forces. Cell Commun Adhes 17(2):48–54

Dinca V, Ranella A, Popescu A, Dinescu M, Farsari M, Fotakis C (2007) Parameters optimization for biological molecules patterning using 248-nm ultrafast lasers. Appl Surf Sci 254:1164–1168

Dinca V, Farsari M, Kafetzopoulos D, Popescu A, Dinescu M, Fotakis C (2008) Patterning parameters for biomolecules microarrays constructed with nanosecond and femtosecond UV lasers. Thin Solid Films 516:6504–6511

Discher DE, Mooney DJ, Zandstra PW (2009) Growth factors, matrices, and forces combine and control stem cells. Science 324:1673

Duocastella M, Fernández-Pradas JM, Morenza JL, Serra P (2010a) Sessile droplet formation in the laser-induced forward transfer of liquids: a time-resolved imaging study. Thin Solid Films 518:5321–5325

Duocastella M, Patrascioiu A, Fernández-Pradas JM, Morenza JL, Serra P (2010b) Film-free laser forward printing of transparent and weakly absorbing liquids. Opt Express 18(21):21815–21825

Fernandes TG, Diogo MM, Clark DS, Dordick JS, Cabral JMS (2009) High-throughput cellular microarray platforms: applications in drug discovery, toxicology and stem cell research. Trends Biotechnol 27(6):342

Gaebel R, Ma N, Liu J, Guan J, Koch L, Klopsch C, Gruene M, Toelk A, Wang W, Mark P, Wang F, Chichkov B, Li W, Steinhoff G (2011) Patterning human stem cells and endothelial cells with laser printing for cardiac regeneration. Biomaterials 32:9218–9230

Gruene M, Unger C, Koch L, Deiwick A, Chichkov B (2011a) Dispensing pico to nanolitre of a natural hydrogel by laser-assisted bioprinting. Biomed Eng Online 10:19

Gruene M, Deiwick A, Koch L, Schlie S, Unger C, Hofmann N, Bernemann I, Glasmacher B, Chichkov B (2011b) Laser printing of stem cells for biofabrication of scaffold-free autologous grafts. Tissue Eng Part C Methods 17:79–87

Gruene M, Pflaum M, Deiwick A, Koch L, Schlie S, Unger C, Wilhelmi M, Haverich A, Chichkov B (2011c) Adipogenic differentiation of laser-printed 3D tissue grafts consisting of human adipose-derived stem cells. Biofabrication 3:015005

Gruene M, Pflaum M, Hess C, Diamantouros S, Schlie S, Deiwick A, Koch L, Wilhelmi M, Jockenhoevel S, Haverich A, Chichkov B (2011d) Laser printing of three-dimensional multicellular arrays for studies of cell-cell and cell-environment interactions. Tissue Eng Part C Methods 17(10):973–982

Hellström M, Kalén M, Lindahl P, Abramsson A, Betsholtz C (1999) Role of PDGF-B and PDGFR-beta in recruitment of vascular smooth muscle cells and pericytes during embryonic blood vessel formation in the mouse. Development 126:3047

Hon KKB, Li L, Hutchings IM (2008) Direct writing technology-advances and developments. CIRP Ann 57:601–620

Hopp B, Smausz T, Kresz N, Barna N, Bor Z, Kolozsvari L, Chrisey DB, Szabo A, Nogradi A (2005) Survival and proliferative ability of various living cell types after laser-induced forward transfer. Tissue Eng 11(11-12):1817–1823

Hui TY, Cheung KMC, Cheung WL, Chan D, Chan BP (2008) In Vitro chondrogenic differentiation of human mesenchymal stem cells in collagen microspheres: influence of cell seeding density and collagen concentration. Biomaterials 29:3201

Keriquel V, Guillemot F, Arnault I, Guillotin B, Miraux S, Amédée J, Fricain J-C, Catros S (2010) In vivo bioprinting for computer- and robotic-assisted medical intervention: preliminary study in mice. Biofabrication 2:014101

Klopsch C, Gäbel R, Kaminski A, Mark P, Wang W, Toelk A, Delyagina E, Kleiner G, Koch L, Chichkov B, Mela P, Jockenhoevel S, Ma N, Steinhoff G (2012) Spray- and laser-assisted biomaterial processing for fast and efficient autologous cell-plus-matrix tissue engineering. J Tissue Eng Regen Med 9(12):E177–E190. https://doi.org/10.1002/term.1657 Epub 2012 Dec 4 (2015)

Koch L, Kuhn S, Sorg H, Gruene M, Schlie S, Gaebel R, Polchow B, Reimers K, Stoelting S, Ma N, Vogt PM, Steinhoff G, Chichkov B (2010) Laser printing of skin cells and human stem cells. Tissue Eng Part C Methods 16:847–854

Koch L, Deiwick A, Schlie S, Michael S, Gruene M, Coger V, Zychlinski D, Schambach A, Reimers K, Vogt PM, Chichkov B (2012) Skin tissue generation by laser cell printing. Biotechnol Bioeng 109:1855–1863

Lin Y, Huang Y, Chrisey DB (2009) Droplet formation in matrix-assisted pulsed-laser evaporation direct writing of glycerol-water solution. J Appl Phys 105(9):093111

Lin Y, Huang Y, Chrisey DB (2011) Metallic foil-assisted laser cell printing. J Biomech Eng 133:025001

Linge C (2004) Establishment and maintenance of normal human keratinocyte cultures. In: Picot J (ed) Methods in molecular medicine, vol 107, Human cell culture protocols. Humana Press, Totowa, p 1

Merfeld-Clauss S, Gollahalli N, March KL, Traktuev DO (2010) Adipose tissue progenitor cells directly interact with endothelial cells to induce vascular network formation. Tissue Eng Part A 16(9):2953

Mese G, Richard G, White TW (2007) Gap junctions: basic structure and function. J Invest Dermatol 127:2516–2524

Michael S, Sorg H, Peck C-T, Koch L, Deiwick A, Chichkov B, Vogt PM, Reimers K (2013) Tissue engineered skin substitutes created by laser-assisted bioprinting form skin-like structures in the dorsal skin fold chamber in mice. PLoS One 8(3):e57741

Mirsky N, Cohen Y (1995) VEGF and ECGF induce directed migration of endothelial cells: qualitative and quantitative assay. Endothelium 255:5444

Niessen CM (2007) Tight junctions/adherens junctions: basic structure and function. J Invest Dermatol 127:2525–2532

Odde DJ, Renn MJ (1999) Laser-guided direct writing for applications in biotechnology. Trends Biotechnol 17:385–389

Othon CM, Wu X, Anders JJ, Ringeisen BR (2008) Single-cell printing to form three-dimensional lines of olfactory ensheathing cells. Biomed Mater 3:034101. https://doi.org/10.1088/1748-6041/3/3/034101

Ovsianikov A, Gruene M, Pflaum M, Koch L, Maiorana F, Wilhelmi M, Haverich A, Chichkov B (2010) Laser printing of cells into 3D scaffolds. Biofabrication 2:014104

Palla-Papavlu A, Paraico I, Shaw-Stewart J, Dinca V, Savopol T, Kovacs E, Lippert T, Wokaun A, Dinescu M (2011) Liposome micropatterning based on laser-induced forward transfer. Appl Phys A 102(3):651–659

Pirlo RK, Wu P, Liu J, Ringeisen B (2011) PLGA/hydrogel biopapers as a stackable substrate for printing HUVEC networks via BioLP™. Biotechnol Bioeng 109(1):262–273

Richard G (2000) Connexins: a connection with the skin. Exp Dermatol 9:77

Ringeisen BR, Kim H, Barron JA, Krizman DB, Chrisey DB, Jackman S, Auyeung RYC, Spargo BJ (2004) Laser printing of pluripotent embryonal carcinoma cells. Tissue Eng 10(3-4):483–491

Ringeisen BR, Othon CM, Barron JA, Young D, Spargo BJ (2006) Jet-based methods to print living cells. Biotechnol J 1:930–948

Schaeffler A, Buechler C (2007) Concise review: adipose tissue-derived stromal cells – basic and clinical implications for novel cell-based therapies. Stem Cells 25:818–827

Schiele NR, Chrisey DB, Corr DT (2011) Gelatin-based laser direct-write technique for the precise spatial patterning of cells. Tissue Eng Part C 17(3):289–298

Schlie S, Mazur K, Bintig W, Ngezahayo A (2010) Cell cycle dependent regulation of gap junction coupling and apoptosis in GFSHR-17 granulosa cells. J Biomed Sci Eng 3:884–891

Taidi B, Lebernede G, Koch L et al (2016) Colony development of laser printed eukaryotic (yeast and microalga) micro-organisms in co-culture. Int J Bioprint 2(2):146–152. https://doi.org/10.18063/IJB.2016.02.001

Takagi M, Umetsu Y, Fujiwara M, Wakitani S (2007) High inoculation cell density could accelerate the differentiation of human bone marrow mesenchymal stem cells to chondrocyte cells. J Biosci Bioeng 103:98

Unger C, Gruene M, Koch L, Koch J, Chichkov B (2011) Time-resolved imaging of hydrogel printing via laser-induced forward transfer. Appl Phys A 103:271–277

Vogel A, Lorenz K, Horneffer V, Hüttmann G, von Smolinski D, Gebert A (2007) Mechanisms of laser-induced dissection and transport of histologic specimens. Biophys J 93:4481–4500

Wu Y, Chen L, Scott PG, Tredget EE (2007) Mesenchymal stem cells enhance wound healing through differentiation and angiogenesis. Stem Cells 25(10):2648

Yan J, Huang Y, Chrisey DB (2013) Laser-assisted printing of alginate long tubes and annular constructs. Biofabrication 5:015002